

# Field Conjugation Adaptive Arrays for Reliable Satellite Downlink Coherent Laser Communications

Aniceto Belmonte<sup>1</sup> and Joseph M. Kahn<sup>2</sup>

1. Technical University of Catalonia, Department of Signal Theory and Communications, 08034 Barcelona, Spain

2. Stanford University, E. L. Ginzton Laboratory, Department of Electrical Engineering, Stanford, CA 94305, USA

[belmonte@tsc.upc.edu](mailto:belmonte@tsc.upc.edu)

**Abstract**— We analyze the performance of adaptive field conjugation array receivers in satellite downlink coherent laser communications. We consider coherent fiber arrays consisting of multiple subapertures, with each subaperture interfaced to a single-mode fiber. We quantify how field conjugation processing improves performance in the presence of turbulence, as compared to a monolithic-aperture coherent receiver having an equal total cross-sectional area. In general, the performance of such a field conjugation adaptive should improve with an increasing number of subapertures and, given a fixed collecting area, the fiber array system can offer superior performance.

**Index Terms**—Free-space coherent optical communications; Channel-matched receivers; Satellite downlinks; Optical ground stations

## I. INTRODUCTION

Optical free-space communication will be a key building block for future information systems in space. Optical-communication links can be used for satellite-to-satellite crosslinks, and up-and-down links between space platforms and aircraft, ships, and other ground platforms. Also, recent advances in coherent optical communications in fiber transmission systems [1] and successful space demonstrations of coherent free-space optical communications indicate that coherent technology is near to be ready for operational deployment. However, when the link includes part of the atmosphere, clear-air turbulence induces serious phase distortions and fading to the coherent link.

In a coherent system, transmitted information can be encoded in the complex electric field, including amplitude, phase and polarization. A coherent receiver measures these degrees of freedom by interfering the received signal with a local oscillator. That said, detection of coherent optical communication through atmospheric turbulence is difficult because atmospheric turbulence can reduce the coherence of the received signal that is to be mixed with the local oscillator. Light propagated through a turbulent atmosphere contains speckle, which will be present at the detector surface. Therefore, illuminating a single-element detector with a uniform LO beam will produce mismatch of the amplitudes and phases of the two fields, resulting in a loss of downconverted power. The downconverted coherent power is maximized when the spatial field of the received signal matches that of the local oscillator. In atmospheric systems, the

phase-compromised beam is superimposed by a perfect local oscillator beam, which results in a very poor overall modulation contrast.

Several techniques can be used to reduce significantly the effects of turbulence in the performance of the coherent communication links. System configurations based on single monolithic apertures using adaptive optical phase compensation to mitigate atmospheric turbulence are being investigated [2]. As an alternative, diversity combining techniques, where signals detected by two or more apertures are combined to reduce the probability of deep fades and improve detection efficiency, are being studied [3-5].

In this work, we consider a coherent channel-matched fiber array receiver consisting of multiple subapertures, with each subaperture interfaced to a single-mode fiber, for improving the performance of an atmospheric downlink coherent system. Instead of using a single monolithic-aperture coherent receiver with a full-size collecting area, a large effective aperture is achieved by combining the output signals from an array of smaller fiber-coupled subapertures (see Fig. 1). Note that if these apertures are sufficiently separated, the fades in different apertures can be considered statistically independent. For close spatial arrangement of the subapertures in a coherent fiber array, atmospheric fading on the array components could be correlated or dependent. In either case, system performance should improve with an increasing number of receivers and, given a fixed collecting area, the fiber array system can offer superior performance.

A coherent channel-matched fiber array offers an advantage in terms of coupling efficiency, as the number of turbulence speckles over each subaperture is much smaller than it would be over a single large aperture. Now, each receiver aperture can be smaller than the scale on which the signal wavefront varies and the local oscillator phase can be matched to the signal to achieve efficient coherent downconversion. Adaptive arrays may be implemented using two options. In electrical combining, optical signals are downconverted separately, and the electrical signals are combined to improve detection statistics. In principle, optical combining is also possible. In this approach, a set of phase shifters is used to co-phase the optical signals from the subapertures prior to combining. Although the main conclusions of the analysis are equally

applicable to optical combining, we focus here on channel-matched adaptive receivers using electrical combining.

First, in Section II, we will consider a general model for the output SNR of a coherent channel-matched fiber array. We will use a statistical description to model the signal collected by the fiber array receiver after propagation through the atmosphere. Then, in Section III, we will analyze the performance of array receivers under the propagation effects of amplitude fluctuations and phase distortions, in addition to local oscillator shot noise.

## II. CHANNEL-MATCHED FIBER ARRAY RECEIVERS

In a coherent communication receiver, the SNR  $\gamma_0$  per unit bandwidth  $B$  for a quantum or shot-noise limited signal can be interpreted as the detected number of photons (photocounts) per symbol, where  $1/B$  is the symbol period. Coherently detected signals are modeled as narrowband RF signals with additive white Gaussian noise (AWGN). For a coherent receiver system, in the presence of atmospheric turbulence, we must consider fading, in which signals are also affected by multiplicative noise. In a fading AWGN channel, we let  $\alpha^2$  denote the atmospheric channel power fading and  $\gamma_0\alpha^2$  denote the instantaneous received SNR per pulse. This quantity is a function of the random channel power fading  $\alpha^2$ , and is therefore random. The statistical properties of the atmospheric random channel fade  $\alpha$ , with probability density function (PDF)  $p_\alpha(\alpha)$ , provide a statistical characterization of the SNR  $\gamma = \gamma_0\alpha^2$ . In this Section we define a statistical model for the fading amplitude  $\alpha$  (i.e., SNR  $\gamma$ ) of the received signal in a fiber array after propagation through the atmosphere.

At this point, it is useful to note that the statistical properties of the atmospheric random channel fade  $\alpha$  are described by a central chi-square distribution [6]

$$p_\alpha(\alpha) = 2(mN)^m \frac{\alpha^{2m-1}}{\Gamma(m)} \exp(-mN\alpha^2) \quad (1)$$

described by parameters  $m$  and  $N$  and where  $\Gamma$  is the complete gamma function. In the presence of turbulence, the received power is scaled by the fading intensity  $\alpha^2$  and the signal is perturbed by AWGN, which is statistically independent of the fading intensity. Hence, the instantaneous SNR  $\gamma$  is proportional to  $\alpha^2$ . Applying the Jacobian of the transformation  $\alpha^2 = \gamma/\gamma_0$  to Eq. (1), the corresponding SNR  $\gamma$  distribution can be described according to a gamma distribution with a shape parameter  $m$  and a mean value  $\bar{\gamma} = \gamma_0\bar{\alpha^2} \equiv \gamma_0/N$  given by

$$p_\gamma(\gamma) = \left(\frac{mN}{\gamma_0}\right)^m \frac{\gamma^{m-1}}{\Gamma(m)} \exp\left(-\frac{mN}{\gamma_0}\gamma\right) \quad (2)$$

Parameters  $m$  and  $N$  are a measure of turbulence effects and, consequently, of the most relevance in our analysis. Here,  $N$  is the inverse of the fading mean-square value and describes the number of field coherent areas (speckles) in the receiver  $l$ th subaperture affecting the fading measurement. The parameter  $m$ , by characterizing the amount of fading through the normalized SNR  $\gamma_l$  variance, gives a complete description of the turbulence fading. When  $m \rightarrow 1$  and the number of

contribution coherent areas  $N$  is large, the normalized variance is unity, as expected for an exponential distribution. When  $m \rightarrow \infty$ , and a very small number of coherent terms  $N$  add together, the normalized variance decreases. Now, the density function becomes highly peaked around the mean value  $\bar{\gamma} = \gamma_0/N$  and there is only weak fading to be considered.

In a field conjugation fiber array, the downconverted electrical signals at the output of the single-mode fibers need to be adaptively co-phased and scaled before they are summed, to lessen fading caused by atmospheric turbulence and compensate for imperfect fiber coupling efficiency (see Fig. 1). That is equivalent to maximal-ratio combining of the signals from the array subapertures, considering them to be branches of a diversity receiver [7] and the instantaneous array combiner SNR  $\gamma$  is the sum of the array element SNRs. For independent subaperture signals and equal average branch SNRs, the PDF of the received SNR  $\gamma$  at the output of a perfect  $L$ -branch coherent array can be described as a sum of  $L$  independent and identically distributed gamma random variables. Thus, the random variable  $\gamma$  is also described by the gamma distribution Eq. (2) with a shape parameter ( $mL$ ).

## III. PERFORMANCE OF A DOWN-LINK ARRAY RECEIVER

The purpose of this study is to provide measures of performance related to practical channel-matched downlink receivers of interest in atmospheric coherent detection requiring adaptive compensation. These measures here serve to illustrate the various possibilities that exist on the array optical communication system design. We show the effect of atmospheric turbulence on downlink coherent detection using four basic performance measurements, namely, average SNR; uncertainty of the SNR, also called amount of fading; SNR outage probability; average outage (fade) duration; and the closely related average level crossing rate or frequency of outages [8]. We study the measures as a function of two basic system parameters, i.e., the total equivalent receiver aperture diameter  $D$  and the number of independent branches or subapertures  $L$  in the optical array.

In this analysis, we will consider that the strength of atmospheric turbulence for the downlink channels is defined with the turbulence structure constant  $C_n^2$  profile associated with the Hufnagel-Valley (H-V) model. The H-V model depends on two parameters,  $C_{n0}^2$  and  $V$ . Values of the structure constant at the ground  $C_{n0}^2$  in mountain plateaus generally vary between  $10^{-15}$  and  $10^{-13} m^{-2/3}$ , the latter of which could be considered strong turbulence. The parameter  $V$  is the rms high-altitude windspeed in  $m/s$ .

The profile of  $C_n^2$  defines the effects of turbulence in optical propagation [9,10]. Here, turbulence effects will be quantified by two statistical parameters: the phase coherence diameter  $r_0$  and the scintillation index  $\sigma_I^2$ . We will need them to describe the distribution parameters  $m$  and  $N$  expressing turbulence effects in our statistical models. The downlink atmospheric coherence diameter  $r_0$  of a plane wave characterizes the effective seeing angle  $\lambda/r_0$  due to turbulence, where  $\lambda$  is the working wavelength of the link. The parameter  $C_{n0}^2$  affects the  $r_0$  profiles but they are mostly independent of high-altitude

wind speed  $V$ . Coherent diameter  $r_0$  ranges from just a couple of centimeters at low elevation angles to almost 20 cm on a downlink path under small zenith angles and weak turbulence conditions. The downlink atmospheric irradiance variance  $\sigma_1^2$  of a plane wave describe the turbulence power scintillation. Wind speed  $V$  affects the  $\sigma_1^2$  profiles but they are mostly independent of the parameter  $C_{n0}^2$ . In this model,  $\sigma_1^2$  ranges from values below  $\sigma_1^2 = 0.1$ , corresponding to relatively low scintillation levels, to values over  $\sigma_1^2 = 0.7$ , corresponding to strong scintillation but still below the saturation regime. In most practical free-space downlinks, amplitude fluctuations are not saturated.

Of the several possible performance measures that exist, the signal-to-noise ratio (SNR) is typically the easiest to evaluate and most often serves as an excellent indicator of the overall fidelity of the system. While traditionally the term “noise” in signal- to-noise ratio refers to the ever-present thermal noise at the input to the receiver, in the context of a communication system subject to fading impairment, the more appropriate performance measure is average SNR:

$$\bar{\gamma} = \int_0^{\infty} \gamma p_{\gamma}(\gamma) d\gamma \quad (3)$$

Here  $p_{\gamma}(\gamma)$  denotes the gamma probability density function (PDF) of  $\gamma$ . Figure 2 shows the average SNR  $\bar{\gamma}$  as a function of telescope diameter  $D$  for a structure constant  $C_{n0}^2 = 10^{-14} m^{-2/3}$  and elevation angle  $\theta = 30^\circ$  are considered. The SNR has been normalized by the turbulence-free SNR per symbol  $\gamma_0$ , i.e.  $\bar{\gamma}/\gamma_0$ . In essence, this is the fading mean square value  $\bar{\alpha}^2 = 1/N$  that, in our modeling, describes the effective number of field coherent areas affecting the fading measurement.

SNR is shown for different numbers of supapertures  $L$  in a coherent array (see Fig. 1). The case  $L = 1$  corresponds to a monolithic aperture (blue lines). When no receive diversity is considered,  $D$  equals the receiver aperture diameter. The area  $\pi D^2$  describes the combined, multi-aperture system equivalent aperture and each receiver has a pupil area  $1/L$  times the pupil area of the single receiver system so that the received signal power in both the single and multiple receiver systems is the same. The analysis also considers an optical fiber coupling-geometry parameter  $\tau$  for each subaperture lens [11]. The truncation parameter of the pupil  $\tau \equiv D/2\omega_m$  describes the ratio of the receiver aperture diameter  $D$  to the diameter of the backpropagated fiber mode  $2\omega_m$ . A large value of  $\tau$  or  $D \gg 2\omega_m$  corresponds to a narrow Gaussian mode or a weakly truncated pupil. A uniformly illuminated pupil is obtained by letting  $\tau \rightarrow 0$ . The truncation parameter  $\tau$  describes the coupling geometry of the array and must be chosen to optimize the receiving system performance. Although the optimal truncation parameter may depend on the level of atmospheric turbulence considered, this dependency is very weak, and it is reasonable to choose a value  $\tau = 1.12$ , which is optimal in the absence of turbulence, when the incident plane wave is fully coherent. The same value of the truncation parameter  $\tau$  is used for each subaperture lens and for the single, larger lens.

Note the diminishing returns that are obtained as the number of branches increases. Although as we increase  $L$  the SNR improves appreciably, the greatest improvement is still obtained in going from single- to two-branch combining. In any case, the gain of the array receiver is noticeable. For instances, a multiple receiver system with just  $L=7$  apertures can reach a SNR gain of over 7 dB when compared with a single, monolithic aperture in most situations considered in this analysis.

The average SNR performance criterion does not capture all the channel-matched array benefits. Indeed, if the array advantage were limited to an average SNR gain, then this could be achieved by simply increasing the transmitter power. Of more importance is the aptitude of adaptive array systems to reduce the fading-induced fluctuations or equivalently, in statistical terms, to reduce the relative uncertainty  $\sigma_{\gamma}$  of the signal envelope that cannot be achieved just by increasing the transmitter power. Thus, in order to capture this effect, the fading uncertainty

$$F = \frac{\sigma_{\gamma}}{\bar{\gamma}} \quad (4)$$

is another performance measure that is most often simple to compute and requires knowledge of only the first and second moments of the instantaneous SNR. Note that  $F^2$  is the parameter  $m$  characterizing the amount of atmospheric fading (normalized variance) in our statistical modeling. Because the uncertainty  $F$  is computed at the output of the array, its evaluation will reflect the behavior of the particular diversity combining technique as well as the statistics of the fading channel and thus, as mentioned above, is a measure of the performance of the entire system.

In Fig. 3, fading uncertainty  $\sigma_{\gamma}/\bar{\gamma}$ , in dB, as a function of telescope diameter  $D$ . All considerations on system and atmospheric parameters, as described for Fig. 4, also apply here. As expected for array systems where the fades in different apertures can be considered statistically independent, fading uncertainties decreases with the root square of the number of subapertures, i.e.  $\sqrt{L}$ . This way, as it can be observed in Fig. 3, a 7-branch matched-array may afford a fading reduction of almost 10 dB.

Another standard performance criterion characteristic of diversity systems operating over fading channels is the so-called outage probability and defined as the probability that the instantaneous error probability exceeds a specified value or, equivalently, the probability that the output SNR  $\gamma$  falls below a certain specified threshold,  $\gamma_{th}$ :

$$p_{out} = \int_0^{\gamma_{th}} p_{\gamma}(\gamma) d\gamma \quad (5)$$

The outage probability (fractional fade time or probability of miss) is the cumulative distribution function CDF of  $\gamma$  evaluated at  $\gamma = \gamma_{th}$ . Figure 4 depicts outage probability  $p_{out}$  as a function of threshold parameter  $\gamma_{th}$  indicating outage. The threshold parameter in Fig. 4 normalizes the SNR threshold  $\gamma_{th}$  by the SNR in the absence of turbulence  $\gamma_0$ . Again, all considerations on system and atmospheric parameters on Figs. 2 and 3 apply here, too. The advantages of

using channel-matched arrays are obvious in Fig. 4. A simple 7-branch array is able to have fractional fades of just  $p_{out}=0.01$  even for high SNR thresholds.

In most free-space communication systems, in addition to the previous performance measures, the frequency of outages and the average outage (fade) duration are important performance criteria for the proper selection of the transmission symbol rate, interleaver depth, or time slot duration. As discussed before, an outage is declared whenever the output SNR  $\gamma$  falls below a predetermined threshold  $\gamma_{th}$ . The average outage duration,  $\tau(\gamma_{th})$  (in seconds) is a measure of how long, on the average, the system remains in the outage state and is given by

$$\tau(\gamma_{th}) = \frac{p_{out}}{N(\gamma_{th})} \quad (6)$$

Here, the outage probability  $p_{out}$  is divided by the frequency of outages  $N(\gamma_{th})$ , i.e., the average level crossing rate of the output SNR  $\gamma$  at level  $\gamma_{th}$ . It can be obtained from the well-known Rice formula for the joint PDF of  $\gamma$  and its time derivative  $\dot{\gamma}$  for the gamma distribution used in this analysis. It measures the expected number of fades (surges) per second as the number of negative (positive) crossings below the specified threshold level  $\gamma_{th}$ .

Figure 5 shows the average fade duration (mean outage time) as a function of the threshold parameter. The threshold parameter normalizes the SNR threshold  $\gamma_{th}$  indicating outage by the SNR in the absence of turbulence  $\gamma_0$ . A standard atmospheric channel bandwidth (frequency) of  $f_0 = 500$  Hz has been considered. The atmospheric frequency  $f_0$  provides a measure of the effective bandwidth of the coherent signal fluctuations. Although this frequency in general should be defined in terms of the temporal correlation properties of the coherent signal, we set it to a value which we could consider as typical of many atmospheric scenarios of moderate-to-strong turbulence. The frequency  $f_0$  affects the expected number of fades and the mean fade time, but does not have any effect on the probability of fade (outage probability). Once again, as depicted in Fig. 5, a relatively small channel-matched array with 7 subapertures can reduce mean outage times by a factor of 10 in most practical situations. The corresponding frequency of outages goes down very quickly when the considered outage SNR threshold is just -20 dB below the expected turbulence-free SNR  $\gamma_0$ .

Details of our analysis and extended results will be presented at the meeting.

#### ACKNOWLEDGMENT

The research of Aniceto Belmonte was funded by the European Space Agency ESA/ESTEC P.O. Ref. 5401000780 and the Spanish Department of Science and Innovation MICINN Grant No. TEC 2009-10025.

#### REFERENCES

1. G. Li, "Recent advances in coherent optical communication," *Adv. Opt. Photon.* **1**, 279-307 (2009).
2. A. Belmonte and J. M. Kahn, "Performance of synchronous optical receivers using atmospheric compensation techniques," *Opt. Express* **16**, 14151-14162 (2008).
3. H. G. Sandalidis, T. A. Tsiftsis, and G. K. Karagiannidis, "Optical wireless communications with heterodyne detection over turbulence channels with pointing errors," *J. Lightwave Technol.* **27**, 4440-4445 (2009).
4. E. J. Lee and V. W. Chan, "Diversity Coherent and Incoherent Receivers for Free-Space Optical Communication in the Presence and Absence of Interference," *J. Opt. Commun. Netw.* **1**, 463-483 (2009).
5. A. Belmonte and J. M. Kahn, "Capacity of coherent free-space optical links using diversity-combining techniques," *Opt. Express* **17**, 12601-12611 (2009).
6. M. Nakagami, "The m-distribution. A general formula of intensity distribution of rapid fading," in *Statistical Methods in Radio Wave Propagation*, W. C. Hoffman, ed. (Pergamon Press, 1960).
7. J. D. Parsons, "Diversity techniques in communications receivers," in *Advanced Signal Processing*, D. A. Creasey, ed. (Peregrinus, 1985), Chap. 6.
8. R. M. Gagliardi and S. Karp, *Optical Communications*, 2nd ed. (John Wiley & Sons, New York, 1995).
9. L. C. Andrews and R. L. Phillips, *Laser Beam Propagation through Random Media* (SPIE Optical Engineering Press, Bellingham, 1998).
10. D. L. Fried, "Optical heterodyne detection of an atmospherically distorted signal wave front," *Proc. IEEE* **55**, 57-67 (1967).
11. P. J. Winzer and W. R. Leeb, "Fiber coupling efficiency for random light and its applications to lidar," *Opt. Letters* **23**, 986-988 (1998).

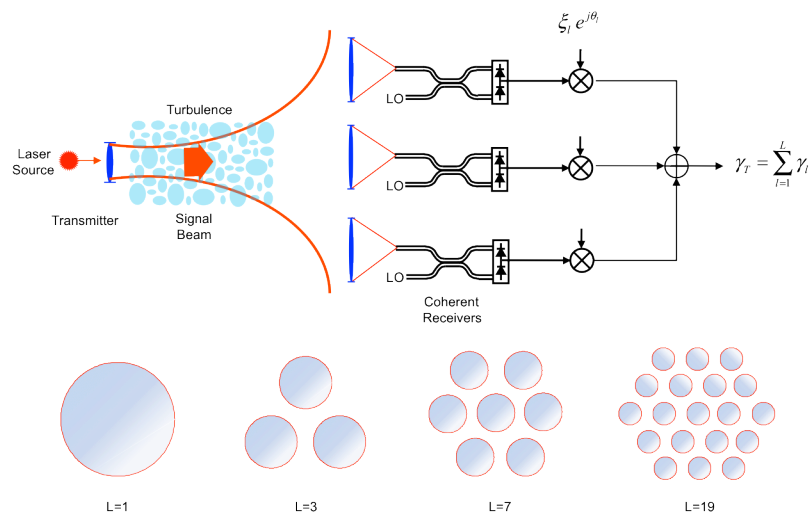


Fig. 1. Adaptive, channel-matched fiber array receivers with different numbers of supapertures  $L$  are considered to mitigate the impact of atmospheric turbulence. The case  $L = 1$  corresponds to a monolithic aperture with diameter  $D$ . The area  $\pi D^2/4$  also describes the combined,  $L$ -branch multi-aperture system equivalent area.

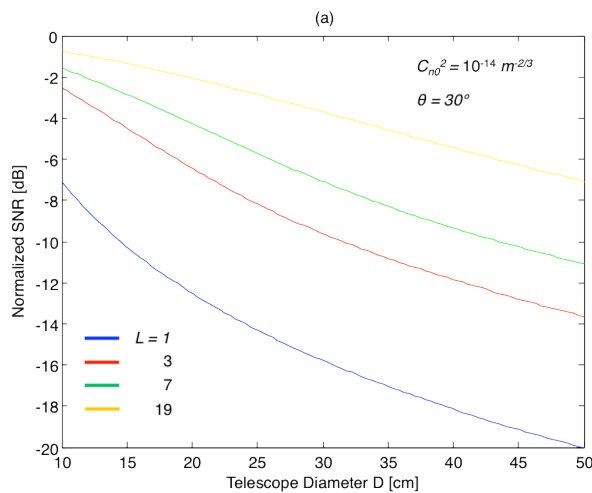


Fig. 2. Average signal-to-noise ratio SNR (detected photons)  $\bar{\gamma}$  as a function of telescope diameter  $D$ . The SNR has been normalized by the turbulence-free SNR per symbol  $\gamma_0$ . Performance is shown for different numbers of of supapertures  $L$  in the channel-matched array receiver.

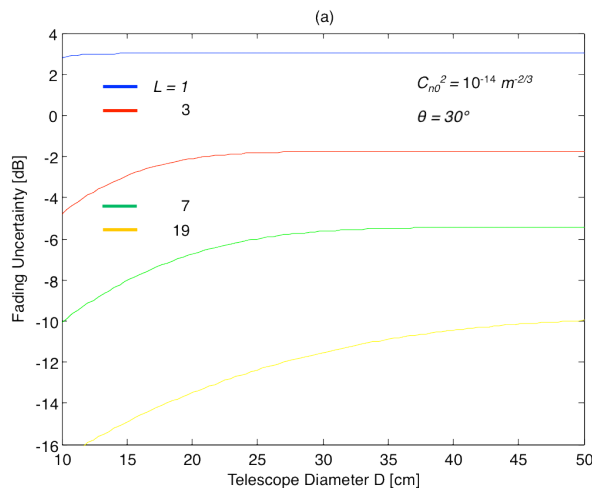


Fig. 3. Fading uncertainty  $\sigma_{\bar{\gamma}}/\bar{\gamma}$ , in dB, as a function of telescope diameter  $D$ . Performance is shown for different numbers of supapertures  $L$  in the channel-matched array receiver.

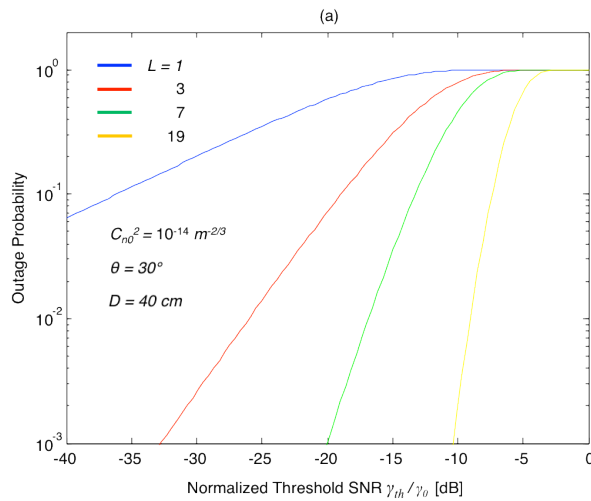


Fig. 4. Outage probability describing the probability that the output SNR falls below a certain specified SNR threshold  $\gamma_{th}$  as a function of a threshold parameter. The threshold parameter in (a) normalizes the SNR threshold  $\gamma_{th}$  indicating outage by the SNR in the absence of turbulence  $\gamma_0$ . Performance is shown for different numbers of of supapertures  $L$  in the array receiver.

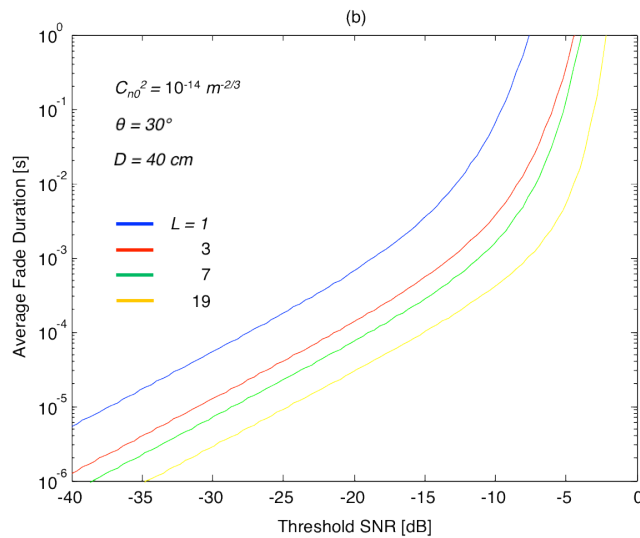


Fig. 5. Average fade duration (mean outage time) as a function of the threshold parameter. The threshold parameter normalizes the SNR threshold  $\gamma_{th}$  indicating outage by the SNR in the absence of turbulence  $\gamma_0$ . A standard atmospheric channel bandwidth (frequency) of  $f_0 = 500 Hz$  has been considered. Performance is shown for different numbers of of supapertures  $L$  in the channel-matched array receiver.